# Dynamic Contrast-Enhanced MRI Measurements of Passive Permeability through Blood Retinal Barrier in Diabetic Rats

*Bruce A. Berkowitz,*[1,2] *Robin Roberts,*[1] *Hongmei Luan,*[1] *Jamie Peysakhov,*[1] *Xianzhi Mao,*[3] *and Kenneth A. Thomas*[3]

**Purpose.** To test the hypothesis that dynamic contrast-enhanced magnetic resonance imaging (DCE-MRI) provides a useful in vivo measure of passive blood retinal barrier permeability surface area product (BRB PS) in experimental diabetic retinopathy.

**Methods.** BRB PS ($cm^3$/min) was measured using DCE-MRI and Gd-DTPA (MW 590 Da) in urethane-anesthetized control rats, sodium iodate–treated rats, rats receiving intravitreally injected human serum albumin (HSA) or vascular endothelial growth factor/vascular permeability factor (VEGF/VPF), or in rats that were diabetic for 2, 4, 6, or 8 months.

**Results.** Sodium iodate–treated rats exhibited an eightfold increase ($P < 0.05$) in BRB PS compared to that in control animals. Furthermore, in iodate-treated rats, the average vitreous signal enhancement was linearly dependant on Gd-DTPA dose ($r = 0.91$, $P < 0.0001$). Six hours postinjection, VEGF/VPF-treated rats exhibited a threefold increase in BRB PS ($P < 0.05$) compared to eyes injected with HSA. In 2-, 4-, and 6-month diabetic rats, BRB PS was not significantly different ($P > 0.05$) from control BRB PS values. After 8 months of diabetes, a twofold increase ($P < 0.05$) in PS over control PS values was found. DCE-MRI demonstrated that the BRB becomes leaky immediately before death, possibly causing an artificial increase in retinal permeability in methods that require enucleation or retinal isolation to assess permeability.

**Conclusions.** DCE-MRI provides a sensitive, noninvasive, and linear assay that accurately measures, without potential artifacts associated with death and enucleation, passive BRB PS in experimental diabetes. DCE-MRI BRB PS measurements are expected to provide a useful surrogate marker of drug treatment efficacy. (*Invest Ophthalmol Vis Sci.* 2004;45:2391–2398) DOI: 10.1167/iovs.03-1381

In patients with diabetes, substantial vision loss is associated with fluid build up in the macula.[1] This diabetic macular edema (DME) is thought to result from breakdown of the blood–retinal barrier (BRB) and subsequent movement of more electrolytes and water into than out of the macula.[2] Current treatment of DME typically involves focal photocoagulation. However, this strategy is destructive and not always effective.[2] A better understanding of the timing of leakage and mechanisms associated with BRB breakdown is expected to facilitate the development of better therapies for DME.

Unfortunately, fundamental questions continue regarding the temporal evolution and extent of damage to BRB as a function of diabetes duration. One reason is that a wide range of techniques have been used by different laboratories and many of these approaches do not provide measures of BRB damage as quantitative physiologic parameters [e.g., permeability surface area product (PS), units $cm^3$/min]. Because it is not possible to measure permeability changes separate from alterations in surface area, the product of the two (PS) is commonly used in physiological investigations of tissue leakiness.[3] PS is the unidirectional in-flow rate of tracer (mM/min) per unit concentration difference across the damaged BRB ($mM/cm^3$).[3] Many preclinical studies have reported increased retinal levels of probes, such as albumin (66 kDa) and Evans blue dye (which rapidly associates with plasma albumin) as evidence for increased BRB damage in as early as 2 weeks of diabetes.[4–8] In contrast, studies involving other tracers, such as sucrose (342 Da), found little to no early increase in passive BRB PS.[5,9–12] Detection of diabetes-related changes in BRB permeability appears to depend on the size and properties of the probe.[5] In addition, the methods used to evaluate BRB damage in the studies often require animal death and/or enucleation and so cannot be used clinically. It is not yet known if the procedures of animal death and/or enucleation produce a potentially confounding BRB opening artifact as the animal approaches death and energy resources are used up.

In patients with nonproliferative diabetic retinopathy there is a strong association between increased *passive* (i.e., between tight cell–cell junctions) permeability to fluorescein (390 Da) through the BRB and leakage on fluorescein angiography, visual acuity, and different stages of DME.[13–15] These results strongly support monitoring increased passive BRB permeability to small molecular weight probes as a useful surrogate marker of increased risk of edema formation.[2] However, interpretation of the results of vitreous fluorometry can be confounded by factors such as active outward transport from the vitreous, poorly defined fluorescein pharmacokinetics, rapid metabolic conversion to fluorescein glucuronide (which fluoresces over a similar wavelength as fluorescein), and plasma protein binding of fluorescein, that can cause misinterpretation of the data in terms of BRB passive permeability.[16–18] Because vitreous fluorophotometry is a one-dimensional optical approach and requires a clear optic medium, its application is limited to patients without vitreous liquefaction and media opacities.[15] As a result, fluorophotometry measurements of BRB damage often are possible only in a subset of diabetic patients.[15] There is a need for routine, nondestructive, multidimensional assessment of increased passive BRB permeability that can be applied in the clinic and in preclinical models.

From the [1]Department of Anatomy and Cell Biology, Wayne State University, Detroit, Michigan; [2]Kresge Eye Institute, Wayne State University, Detroit, Michigan; and [3]Department of Cancer Research, Merck Research Laboratories, West Point, Pennsylvania.

Supported by National Institutes of Health Grant EY10221 and Merck & Co.

Submitted for publication December 19, 2003; revised February 25, 2004; accepted March 19, 2004.

Disclosure: **B.A. Berkowitz**, Merck & Co. (C, F); **R. Roberts**, None; **H. Luan**, None; **J. Peysakhov**, None; **X. Mao**, Merck & Co. (E); **K.A. Thomas**, Merck & Co. (E)

The publication costs of this article were defrayed in part by page charge payment. This article must therefore be marked "*advertisement*" in accordance with 18 U.S.C. §1734 solely to indicate this fact.

Corresponding author: Bruce A. Berkowitz, Department of Anatomy and Cell Biology, Wayne State University School of Medicine, 540 E. Canfield, Detroit, Michigan 48201; baberko@med.wayne.edu.

Previously a rapid method for measuring BRB PS in patients with proliferative diabetic retinopathy and in a variety of preclinical models was developed, validated, and applied using dynamic contrast MRI (DCE-MRI) and the clinically available, small molecular weight contrast agent gadolinium-diethylenetriamine pentaacetic acid (Gd-DTPA; 590 Da).[19–27] As opposed to fluorescein, Gd-DTPA is not actively transported from the vitreous, has a well-defined pharmacokinetic profile, is not metabolized, does not bind to plasma proteins, will cross BRB only after disruption of tight cell junctions (i.e., is a passive permeability tracer), and can be used to provide an accurate measure of BRB PS.[25,26] Also, DCE-MRI does not require a clear optic medium, provides a noninvasive, high resolution two-dimensional map of the location of the influx of contrast agent into the vitreous (e.g., from the retina or iris/ciliary body), and is clinically applicable.[23,24,26] Furthermore, DCE-MRI data are in visual agreement with fluorescein angiogram in patients with proliferative diabetic retinopathy.[28] These considerations highlight DCE-MRI and Gd-DTPA as a powerful noninvasive approach to study increased passive BRB permeability in both preclinical and clinical subjects with diabetes. However, DCE-MRI studies have not yet been performed in more common experimental models of diabetic retinopathy involving the rat.

This study first determined if DCE-MRI had potential advantages over methods that involve animal death and/or enucleation by measuring BRB opening before, during, and after death. In addition, the sensitivity, linearity, and accuracy of DCE-MRI were evaluated in nondiabetic rats pretreated with sodium iodate (a known retinal pigment epithelial-specific poison[11,26,29–32]) or vascular endothelial growth factor/vascular permeability factor (VEGF/VPF), as well as in diabetic rats (with 2, 4, 6, or 8 months of diabetes).

## METHODS

The animals were treated in accordance with the NIH Guide for the Care and Use of Laboratory Animals and the ARVO Statement on Animals in Vision Research.

### Animal Models

**Sodium Iodate.** Conscious rats were given 30 mg/kg sodium iodate (Sigma, St. Louis, MO) i.p. 24 hours before the MRI examination.[11]

**VPF/VEGF.** Two $\mu$L containing either a human serum albumin (HSA) vehicle or 0.5 $\mu$g VEGF/VPF (R&D Systems, Minneapolis, MN) were injected into the vitreous of anesthetized rats using a 30 g blunt nose needle and a surgical microscope. This bolus dose of VEGF corresponded to a 250 nM initial concentration in the approximately 50 $\mu$L rat vitreous.[33] In VEGF titration studies, this bolus dose was observed to induce rapid and optimal phosphorylation of retinal VEGF receptor 2 (VEGFR2/KDR) in rats (data not shown). Injections were done in a staggered fashion so that each rat was examined by DCE-MRI 6 hours postinjection.

**Diabetes.** The rats in the control group were 2–2.5 months old. To exclude an effect of age on the between-group differences, 8-month-old control rats ($n = 5$) were also studied. Diabetic rats were maintained for 2, 4, 6, or 8 months before being studied. Diabetes was induced in rats (starting weight, 200–220 g; $n = 20$) by injecting streptozotocin (55 mg/kg, 0.05 M citrate buffer, pH 4.5, intraperitoneally) after a 24-hour fast and verified 24 hours later by the presence of hyperglycemia and glucosuria in nonfasting rats. Three animals were excluded from the study due to their hyperglycemia being too mild or the rat being too sick during the 2–6 month period. Animals were fed normal rat chow (5001; Ralston Purina, Richmond, IN) and water ad libitum. Rat urine ketones and glucose and blood glucose levels were monitored daily, and body weight was followed weekly. Subtherapeutic levels of insulin (1–2 U of neutral protamine Hagedorn [NPH] insulin were injected s.c. every day based on the daily measure of blood glucose, and urine volume and ketones) were administered to allow slow weight gain, yet maintain hyperglycemia and glucosuria. Glycosylated hemoglobin was measured 1 week before the MRI examination using a commercial affinity microchromatographic kit (GLYCO-Tek; Helena Laboratories, Beaumont, TX). Final blood glucose levels were measured immediately after the MRI examination.

**MRI Examination.** On the day of the examination, urethane anesthetized animals (0.083 mL of a 36% solution of urethane/20 g animal weight, i.p., freshly made daily; Aldrich, Milwaukee, WI) had their tail vein cannulated with a 25 g catheter. The dose of contrast agent (Gd-DTPA, Magnevist; Berlex Laboratories, Wayne, NJ) was 0.1 mM Gd-DTPA/L/kg. In the sodium iodate–treated rats, a range of Gd-DTPA doses were also investigated (0.01, 0.1, and 0.3 mM Gd-DTPA/L/kg). Rats receiving 0.01 mM GD-DTPA/L/kg were examined immediately afterward using a Gd-DTPA dose of 0.1 mM Gd-DTPA/L/kg to confirm the presence of BRB damage. Note only sodium iodate–treated rats that demonstrated DCE-MRI BRB damage spanning the length of the retina were used in this study. Rats were then gently positioned on an MRI-compatible holder. Rectal temperature was continuously monitored and maintained. MRI data were acquired on a 4.7 T system using a two-turn surface coil (1.5 cm diameter rat) placed over the eye and a spin-echo imaging sequence (repetition time [TR], 1 second; echo time [TE], 22.7 ms; number of acquisitions [NA], 1; matrix size, 128 × 256; slice thickness, 1 mm; field of view, 32 × 32 mm$^2$; sweep width, 25,000 Hz; 2 minutes/image). A capillary tube (1.5 mm inner diameter) filled with distilled water was used as the external standard. Twelve sequential 2-minute images were acquired as follows: three control images before injection of contrast agent and nine images during and after a 6 second Gd-DTPA bolus injection. In other words, images were acquired for up to 18 minutes after injection of Gd-DTPA. For some of the early time point diabetic rats, images were also collected for up to 40 minutes postinjection but no leakage was detected (data not shown). In each animal Gd-DTPA was injected at the same phase encode step collected near the beginning of the fourth image.

At the end of the experiment, blood from the tail vein was collected and analyzed for glucose concentration. After the MRI examination, the animals were humanely killed.

**Death Experiments.** These experiments ($n = 3$) were performed as above except that 0.2 mL of urethane was injected into the tail vein at the end of scans 5 and 7. In other words, Gd-DTPA was allowed to circulate for 4 minutes before the first urethane bolus. Respiratory movement was evident as slight "ghosting" in each image (i.e., low-intensity image smearing in the phase-encode direction). This ghost artifact arises because during respiration, the animal is not in exactly the same spatial location throughout image acquisition. Cessation of this movement was used to assess time of animal death (usually observed by scan 11).

**Data Analysis.** To be included in this study, the animal must have demonstrated minimal eye movement during the MRI examination, nongasping respiratory pattern before and after the MRI examination, and constant rectal temperatures.

To correct for movement within the slice plane, an affine transformation was performed on each animal using software written in-house. An affine transformation applies a linear combination of translation, rotation, scaling and/or shearing (i.e., nonuniform scaling in some directions) operations that preserves lines and parallelism to co-register images to a reference image. Because the slice thickness (1 mm) is relatively large compared to the diameter of the eye (approximately 6 mm), partial volumes will be similar if the eye subtly moves out of the imaging plane and so the data analysis results are not expected to be substantially affected. After co-registration, the MRI data were transferred to a Power Mac G4 computer and analyzed using the program IMAGE (a freeware program available at http://rsb.info.nih.gov/nih-image; last accessed 5/12/04). The three precontrast images were averaged to improve the signal-to-noise ratio. All images were then

normalized to an external standard signal intensity. A small region-of-interest (ROI) in the anterior vitreous was also chosen for normalization to 100 before subtracting out the background noise. The precontrast image was then smoothed twice to reduce noise. For each pixel, the fractional signal enhancement, E, was calculated:

$$E = (S(t) - S_0)/S_0 \quad (1)$$

where $S(t)$ is the pixel signal intensity at time $t$ postcontrast, and $S_0$ is the precontrast signal intensity (measured from the average of the three control images) at the same pixel spatial location. To determine BRB PS, a ROI was chosen on the E map that contained the entire vitreous space. The area of this ROI and the mean E within the ROI were measured at each postcontrast time point. In principle, measurement of PS only requires a single time point after injection (see below), because the greatest difference in E between controls (which do not enhance) and experimental subjects (which may enhance) is expected at the latest time points, only the last four time points (13, 15, 17, and 19 minutes) were converted to BRB PS values. These PS values were then averaged to minimize the influence of noise on any one PS value.

To calculate PS, the Simplified Early Enhancement method of Tofts and Berkowitz was used[3,26] and is briefly described here. This method requires estimates of the vitreous $T_1$ in the absence of Gd-DTPA ($T_{10}$), the relaxivity of Gd-DTPA ($R_1$, $s^{-1}$ $mM^{-1}$), and the Gd-DTPA concentration plasma time course parameters.[3,23,26] Vitreous $T_{10}$ was previously reported to be approximately 3.5 seconds. This value was checked in a control rodent using a homogenous excitation and surface coil reception and collecting gradient recalled echo images at different flip angles. As expected for a $T_{10}$ of approximately 3.5 seconds, a maximum vitreous signal intensity was found at a flip angle of 12°–13° (based on the Ernst angle formula, data not shown).[34] Gd-DTPA relaxivity is constant at a set temperature and field strength and so the previously reported value of 4.5 seconds/mM was used.[26] To determine the pharmacokinetic parameters after a bolus of Gd-DTPA in rats, blood samples were obtained in separate experiments in heparinized tubes during the precontrast period, and 1, 3, 7, 15, 30, and 60 minutes postinjection. These samples were centrifuged and the plasma fraction was obtained for NMR analysis. Inversion recovery $T_1$ experiments were performed on the water signal of the plasma fraction at room temperature. From the $T_1$ value, the amount and thus concentration of Gd-DTPA was determined from a calibration curve obtained at room temperature in a separate phantom study. The unidirectional rate constant, $k$, is given by

$$K = E/R_1T_kD((a_1[1 - \exp(-m_1t)]/m_1) + (a_2[1 - \exp(-m_2t)]/m_2)) \quad (2)$$

where $D$ is the Gd-DTPA dose, $T_k = T_R \exp(-T_R/T_{10})/(1 - \exp(-T_R/T_{10}))$, $T_R$ is the repetition time, $a_{1,2}$ are the Gd-DTPA plasma amplitudes, and $m_{1,2}$ are the rate constants of each plasma component. Thus, $k$ can be found from a single measurement of enhancement, provided $R_1$, $T_k$, and the plasma parameters are known. Setting the vitreous volume in the slice $Vv = A_{\text{region-of-interest}}$(slice thickness), PS then is:

$$PS = kA_{\text{region-of-interest}} \text{ (slice thickness)}. \quad (3)$$

This equation assumes that all tracer in the slice originated from the portion of retina in that slice. This assumption is justified by the results of the present experiments in sodium iodate–treated rats, which demonstrated MRI-derived BRB PS values similar to those previously measured using traditional physiologic methods (see below).

### Statistical Analysis

The data for the PS and glycated hemoglobin parameters were consistent with a normal distribution and presented as mean ± SEM. Comparisons between groups were performed using an ANOVA analysis with $P < 0.05$ considered statistically significant.

**TABLE 1.** Summary of Rat Systemic Physiology

| Group | % Glycated Hemoglobin (Mean ± SEM) |
|---|---|
| Control ($n = 5$) | 3.8 ± 0.1 |
| 2 month Diabetic ($n = 5$) | 9.7 ± 0.3* |
| 4 month Diabetic ($n = 5$) | 11.6 ± 1.1* |
| 6 month Diabetic ($n = 5$) | 8.9 ± 0.8* |
| 8 month Diabetic ($n = 4$) | 10.2 ± 0.7* |

* Compared with Control group, $P < 0.005$.

## RESULTS

### Diabetic Model Characteristics

As expected, compared with control animals, the percent glycated hemoglobin values in all diabetic rats were significantly elevated ($P < 0.05$; Table 1). There was no significant difference ($P > 0.05$) between the percent glycated hemoglobin levels of the four durations of diabetes.

### Plasma Gd-DTPA Time Course

A linear relationship was found between Gd-DTPA concentration and $T_1$ in vitro [$(1/T_1) = 0.37$/seconds + 4.95/seconds/mM*(Gd-DTPA concentration); $r = 0.999$, $P < 0.0001$]. This equation was used to convert the plasma water $T_1$ times after a bolus of contrast agent into Gd-DTPA concentrations. The following Gd-DTPA decay parameters were obtained by fitting to a biexponential function ($r = .99$): $a_1 = 3.19$ kg BW/L, $m_1 = 0.275$/minute, $a_2 = 0.261$ kg BW/L, $m_2 = 0.0096$/minute.

### MRI

Figure 1 illustrates enhancement parameter maps after a bolus injection of Gd-DTPA in control, sodium iodate–treated, HSA-injected control, and VPF/VEGF-injected rats. In sodium iodate–treated rats, a linear relationship ($r = 0.91$, $P < 0.005$) was found between vitreous signal enhancement and dose of Gd-DTPA (Fig. 2). The BRB PS of sodium iodate–treated rats was significantly ($P < 0.005$) greater than that of control rats (Fig. 3). In addition, a threefold increase ($P < 0.05$) in BRB PS was found in VPF/VEGF injected eyes compared with HSA-injected control eyes (Figs. 1 and 3). No significant ($P < 0.05$) differences were found between the BRB PS in noninjected control and HSA-injected eyes (Fig. 3).

Examples of DCE-MRI data for 6- and 8-month diabetic rats are shown in Figure 4. BRB integrity was intact in both 2- and 8-month control groups (data not shown). In the diabetic group, only BRB PS in the 8-month diabetic group was significantly different ($P < 0.05$) from controls (Fig. 5).

### Death

As seen in Figure 6, in control rats, signal intensities change were minimal while the animal was alive ($P > 0.05$), indicating an intact BRB. However, clear evidence for BRB damage ($P < 0.05$) was found before loss of respiratory movement (i.e., death) at 9 minutes postcontrast and later (second arrowhead). BRB opening was also evident within minutes after animal sacrifice by KCl injection (data not shown). Thus, approaching death was associated with a rapid breakdown in BRB permeability.

## DISCUSSION

In this study, for the first time, the utility of DCE-MRI BRB PS measurement using Gd-DTPA in diabetic rats was evaluated. Normally, Gd-DTPA is excluded by the BRB and does not enter

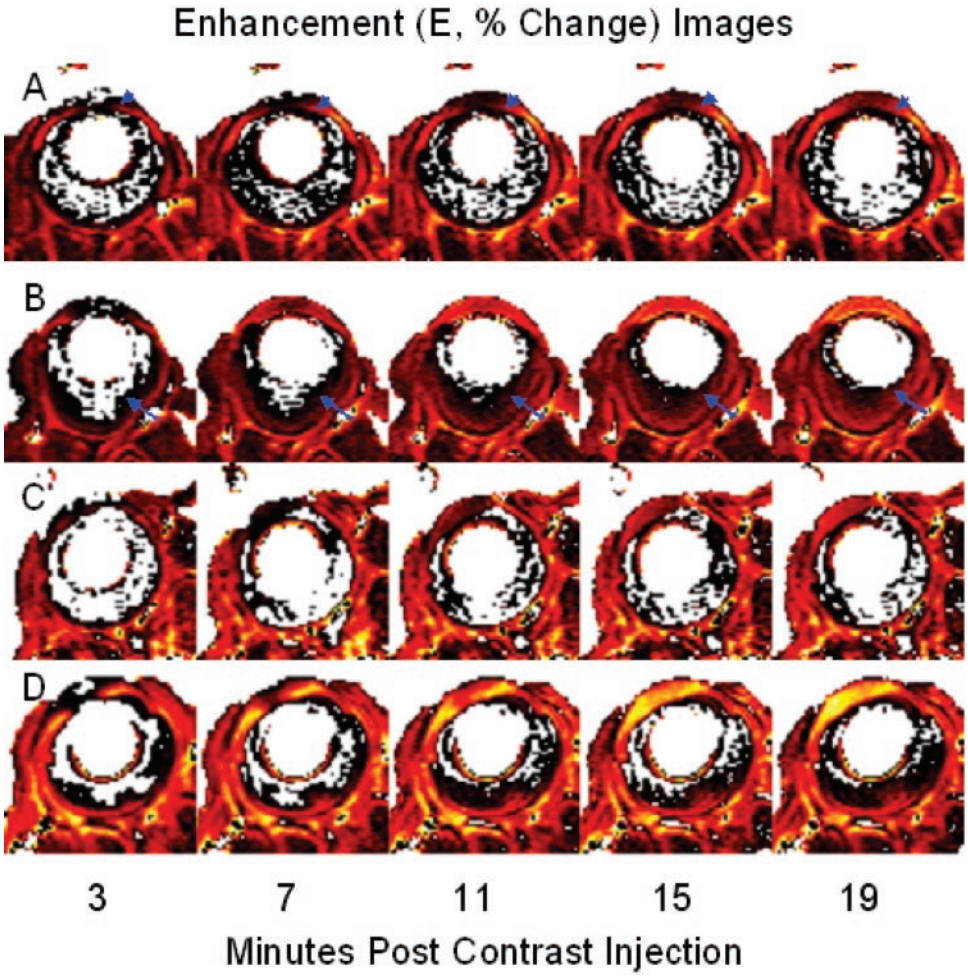


**FIGURE 1.** Parameter maps of the percentage of change in signal intensity (enhancements, E) from precontrast levels at 3, 7, 9, 15, 19 minutes postcontrast injection for representative (**A**) control, (**B**) sodium iodate–treated, (**C**) HSA-injected controls, and (**D**) VPF/VEGF-injected rats. Brighter colors (e.g., *yellow*) represent greater Gd-DTPA levels. *White* is background and represents no change. The same color scale was used for all parameter maps in Figures 1 and 4. The rapid anterior chamber filling (*blue arrowhead*) with contrast agent seen in all animals was expected and was used in each animal to confirm that the injection was good. Note only the sodium iodate– (**B**) and VPF/VEGF-treated (**D**) rats demonstrated coherent increases in vitreous E (*blue arrows*) over time. In addition, in a subset of diabetic rats, postcontrast times up to 40 minutes did not reveal increased vitreous E (data not shown).

the vitreous. When BRB is disrupted, Gd-DTPA enters the vitreous space and strongly influences the surrounding proton spin-lattice relaxation rate ($[T_1]^{-1}$) in direct proportion to the Gd-DTPA concentration.[35] In other words, changes in vitreous MRI signal intensity on a $T_1$ weighted image are a marker of BRB disruption. These signal intensity changes can then be converted into PS.[26] Note that unlike other models in which DCE-MRI can distinguish damage to inner (tight endothelial cell junctions) and outer (tight retinal pigment epithelial junctions) barriers, the situation is not similarly favorable in the rat and

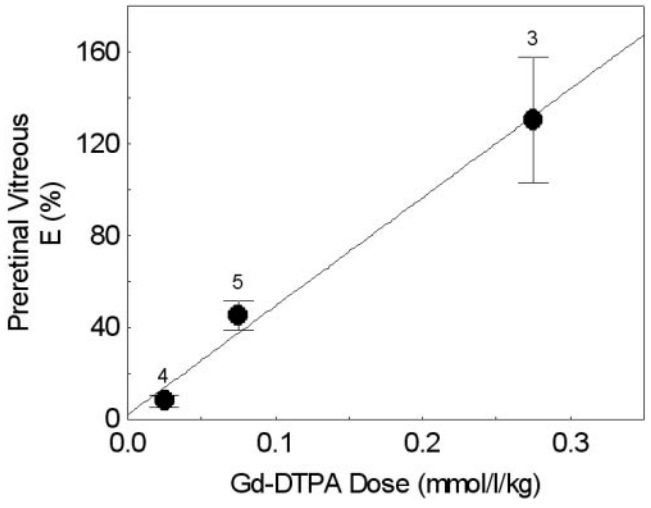


**FIGURE 2.** Plot of the percentage of change in vitreous signal intensity (E) vs. Gd-DTPA dose in sodium iodate–treated rats. A significant linear relationship was found ($r = 0.91$, $P < 0.005$). The numbers of animals used to generate each datum are listed *above* each symbol. Error bars represent the SEM.

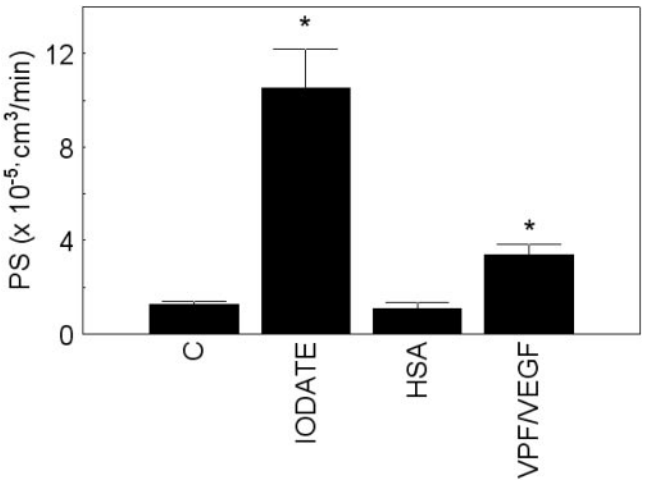


**FIGURE 3.** Summary of BRB PS from control rats (C, $n = 10$), sodium iodate–treated rats (IODATE, $n = 5$), HSA-injected control rats (HSA, $n = 6$), and VPF/VEGF-injected control rats (VPF/VEGF, $n = 13$). Significant difference (*$P < 0.05$) with the control group.

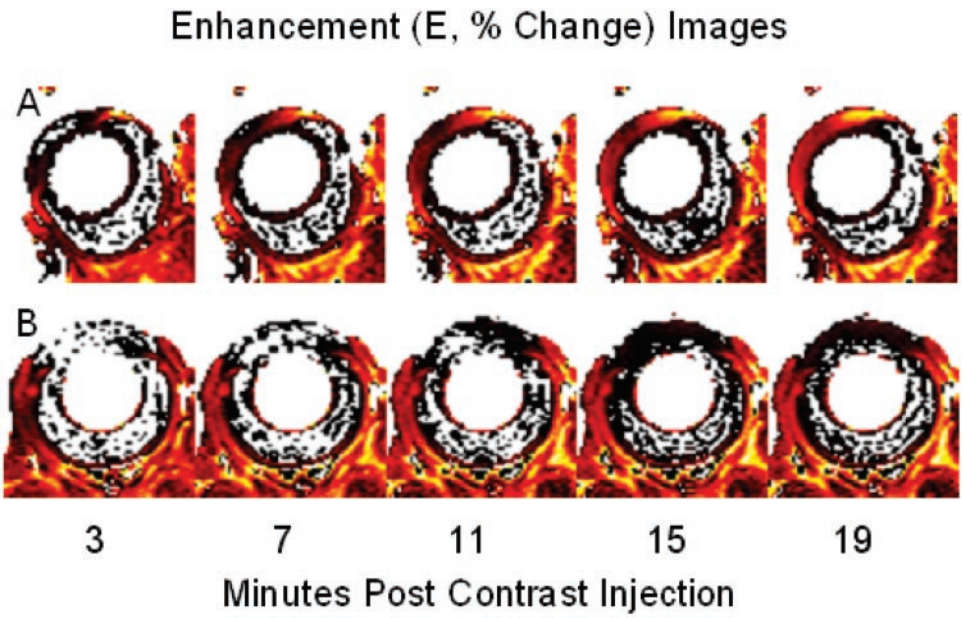


**FIGURE 4.** Parameter maps of the percentage of change in signal intensity (enhancements, E) from precontrast levels at 3, 7, 9, 15, and 19 minutes post 0.1 mM Gd-DTPA/L/kg bolus injection for representative (**A**) 6 months diabetic, and (**B**) 8 months diabetic rats. Brighter colors (e.g., *yellow*) represent greater Gd-DTPA levels. *White* is background and represents no change. Note that only the 8 month diabetic rats showed consistent vitreous E with time. In addition, in a subset of diabetic rats, postcontrast times up to 40 minutes did not reveal increased vitreous E (data not shown).

DCE-MRI cannot resolve the barrier separation.[27] Future investigations may wish to focus on a particular drug treatment and its effect on inner or outer barrier. However, there is a prior need to assess the effect of drug treatment on any measurable BRB damage (i.e., regardless of whether the damage is to the inner or outer barrier) associated with diabetes in the living system. The present study addresses the following fundamental questions that must be answered before questions of inner versus outer barrier are asked: 1) Does any BRB damage exist soon after induction of diabetes? 2) Can BRB damage (inner or outer) be quantitatively measured so as to be potentially useful for assessing drug treatment efficacy in both preclinical and clinical studies? 3) Does the noninvasive method provide additional insight that is different from those obtained by other techniques?

The linearity of DCE-MRI assay was assessed by comparing the injected contrast agent dose to the detected signal in sodium iodate–treated rats. Sodium iodate is not a positive control for the diabetes group because, unlike in diabetes, extensive disruption of the tight cell–cell junctions of the retinal pigment epithelium occurs (within 24 hours posttreatment).[11] Nonetheless, sodium iodate–treated rats are useful for confirming a linear relationship between vitreous E and Gd-DTPA dose (Fig. 2) and for comparing the MRI determined BRB PS to that measured using a more traditional physiological approach. Agreement was found between the DCE-MRI BRB PS ($10.5 \pm 1.7 \times 10^{-5}$ cm$^3$/min) and BRB PS measured by Ennis and Betz[11] ($9.72 \pm 1.86 \times 10^{-5}$ cm$^3$/min) using radiolabeled sucrose (MW 342 Da). The concurrence between these two BRB PS values, given the methodological differences between the studies (e.g., destructive versus nondestructive tissue analysis and different tracers), provides strong support for the underlying assumptions and accuracy of the DCE-MRI approach.

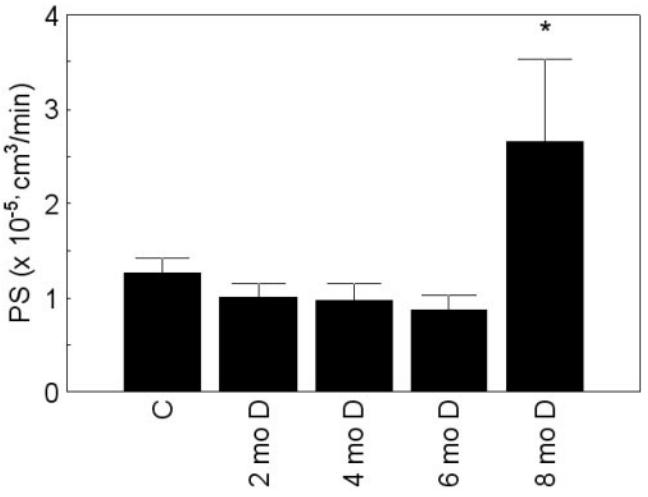


**FIGURE 5.** Summary of BRB PS from control rats ($n = 10$), and 2 months ($n = 5$), 4 months ($n = 5$), 6 months ($n = 5$), and 8 months ($n = 4$) diabetic rats. Significant difference ($^*P < 0.05$) was only found between the control and 8 month diabetic groups.

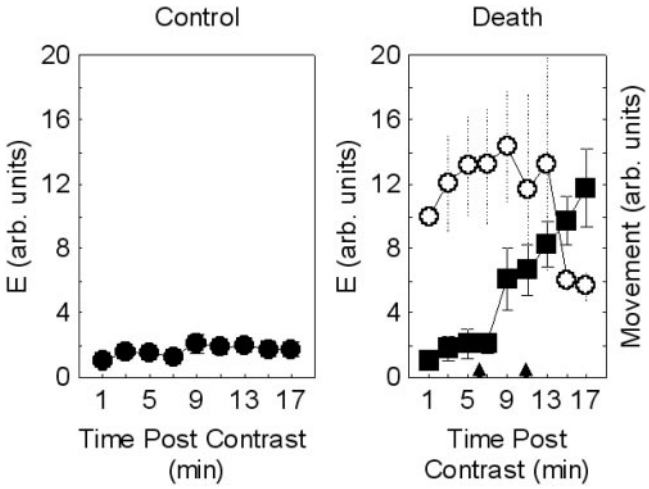


**FIGURE 6.** Plots of vitreous humor % signal enhancement (E, *filled symbols*), normalized to the 1 minute time point value, as a function of time postcontrast injection in control rats ($n = 6$, *left panel*), and control rats receiving two 0.2 mL of additional urethane i.v. (*arrowheads;* $n = 3$, *right panel*). In the *right panel*, respiratory movement (*open circle*), evident as low-intensity image smearing in the phase-encode direction, is also plotted and used to assess time of animal death.

The sensitivity of the DCE-MRI BRB PS measurement to more subtle changes was investigated. A single intravitreous injection of VEGF/VPF is reported to induce a three- to fourfold increase in BRB permeability without disruption of retinal architecture.[36–40] For example, Derevjanik et al.[36] reported evidence of a roughly fourfold increased BRB damage to mannitol (182 Da) 6 hours after intravitreous injection of $10^{-6}$ M VEGF in mice. These findings are supported by the present work, which found a threefold increase in BRB PS in the rat under similar conditions (Fig. 3). Because the dose of VEGF used in the present study was higher than that used in other studies, it might appear that the sensitivity of DCE-MRI is lower. For example, Xu et al.[7] used a tenfold lower dose (50 ng) of VEGF and reported a fourfold increase in BRB leakage. However, based on our calculations (shown below), the VEGF dose used in the present study (and by Derevjanik et al.) and in the work of Xu et al. are both higher than needed to achieve substantial equilibrium binding. Assuming a vitreous volume is 50 $\mu$L in the rat,[41] our VEGF dose of 0.5 $\mu$g corresponded to a vitreous concentration of $0.24 \times 10^{-6}$ M and Xu et al. dose corresponds to a vitreous level of $0.24 \times 10^{-7}$ M. Since the *K*d of VEGF for its two receptors are $\sim 10^{-10}$—$10^{-11}$ M,[42,43] both VEGF doses are clearly higher than needed to achieve substantial equilibrium binding. DCE-MRI BRB PS measurements appear to be a sensitive and quantitative approach for monitoring treatment efficacy on VEGF/VPF-induced BRB damage.

Application of DCE-MRI to diabetic rats revealed increased passive BRB PS only after 8 months of experimental hyperglycemia. It is possible that DCE-MRI is not sensitive enough to detect small increases in vitreous Gd-DTPA that would result from lesser alterations in PS. To estimate the lower limit of BRB damage detectability using the current experimental setup, we note that in control rats, which presumably did not have any BRB damage, vitreous *E* remained constant (i.e., is background noise) over time at a level of 4.6 ± 2.0% (mean ± SD; Fig. 1). It was reasoned that vitreous *E* that is greater than two standard deviations from the mean (i.e., > 2*2% + 4.6% or 8.6%) can be reliably measured. Indeed, changes could be readily detected in vitreous signal intensity of 10.3 ± 2.9% ($n = 5$) in sodium iodate–treated rats after low doses of contrast agent (0.01–0.02 mM Gd-DTPA/L/kg). Converting the minimally detectable vitreous E (8.6%) into a PS value suggested that the sensitivity of the DCE-MRI Gd-DTPA examination appears sufficient to detect increases in BRB PS $> 3.9 \times 10^{-5}$ cm$^3$/min. It appeared that damage of this magnitude did not occur before 8 months of diabetes.

Comparison of the present results in diabetic rats to data in the literature is facilitated by noting that Gd-DTPA (590 Da) has a number of similarities (e.g., it is a nontoxic, nonmetabolized, and passive diffusion tracer (i.e., is not actively transported) with a well-defined plasma time course) to other lower molecular weight radiolabeled tracers [e.g., sucrose (342 Da) and mannitol (344 Da)] that have been used to study BRB damage.[9–12,44] Using other detection methods and these radiolabeled tracers in diabetic or galactose-fed rats, little to no change in passive BRB was found in early diabetes.[9–12,44] In contrast, experiments using other methods and tracers (e.g., fluorescein, albumin, and Evans blue dye) have reported BRB damage as early as 2 weeks after inducing diabetes in rats.[7,8,45–47] Data from Dimattio and Antonetti[4,5] clearly demonstrate that detection of BRB permeability changes in rat models of diabetes is dependent on size and properties of the probe, with smaller molecular weight, strongly hydrophilic tracers being less permeable than larger molecular weight, moderately lipophilic compounds. In addition, as discussed in the Introduction, unambiguous interpretation of increased passive BRB damage after fluorescein injection requires careful attention to a number of potential confounding factors. Further, interpretation of increased albumin-based tracers can also be problematic.[9,48,49]

The present study revealed another potential factor in the contradictory conclusions of studies of diabetes-induced alteration in retinal permeability. The possibility was raised, for the first time, that experimental methods that involve animal death and/or enucleation before determining the extent of BRB damage may in fact be influenced by a BRB opening artifact as the animal approaches death and local energy resources are used up. For example, in studies by Xu et al., [7] the procedure is as follows: Evans blue dye was allowed to circulate for 90 minutes in ketamine/xylazine-anesthetized rats. Then the chest cavity was opened, and rats were perfused via the left ventricle. Note that the pneumothorax produced by opening of the chest cavity will significantly compromise the animal's physiology and soon lead to the animal's death. In addition, pH 3.5 was used because it allowed optimal binding of Evans blue dye to albumin. It is possible that a pH 3.5 solution could produce a change in cell shape and BRB disruption. Nagy, Szabo, and Huttner[50] found that cerebral perfusion with acidic pH buffer induced substantial blood–brain barrier leakage. Preliminary studies (data not shown) also found increasing vitreous signal intensity enhancements (E), at progressively lower arterial pH's. Although more work is needed, it appears possible that the use of low pH wash solutions alone can induce BRB damage. In addition, the rat was then perfused for 2 minutes at a physiological pressure of 120 mm Hg. However, ketamine/xyalzine anesthetic will lower mean arterial blood pressure.[51] The act of perfusing the animal at a physiological pressure of 120 mm Hg might produce a relative acute hypertensive event. Such events are associated with damage to the blood–brain barrier.[52] It is also possible that some dilution of extravascular dye by the perfusate also occurred. Our data raise the possibility that some combination of pneumothorax, acidic flush solution, and in situ perfusion could have artificially induced BRB damage so that some of the EBD leaked into the retina. Unfortunately it is not currently possible to perform the combination of pneumothorax, flush, and in situ cardiac perfusion inside the bore of the magnet. In addition, Evans blue dye rapidly binds to tissue proteins causing the Evans blue dye-derived PS to be dramatically different from that obtained using the standard $^{125}$I-albmin marker.[48] If a similar phenomenon occurs in the retina, then this would decrease the efficiency of vascular dye washout and would introduce an error in the Evan's blue dye method. We speculate that the stress of pneumothorax, low pH, and elevated pressure potentiated rapid VEGF-induced leakage by themselves (i.e., in controls) were not sufficient to produce similar leakage. DCE-MRI avoids these problems and the death artifact. In future studies, DCE-MRI BRB PS measurements are expected to be useful in assessing treatment efficacy in both preclinical and clinical settings.

The present data underscore the power of DCE-MRI to provide a noninvasive measure BRB PS after VPF/VEGF treatment or in experimental diabetes that could be useful for evaluating drug treatment efficacy both in preclinical models as well as in patients clinically.

## *Acknowledgments*

The authors thank Gary Trick and Steven Ennis for helpful discussions and Robert Gould for his encouragement.

## *References*

1. Ferris FL, III, Patz A. Macular edema. A complication of diabetic retinopathy. *Surv Ophthalmol.* 1984;28 Suppl:452–461.
2. Lund-Andersen H. Mechanisms for monitoring changes in retinal status following therapeutic intervention in diabetic retinopathy. *Surv Ophthalmol.* 2002;47 Suppl 2:S270–S277.

3. Tofts PS, Berkowitz BA. Rapid measurement of capillary permeability using the early part of the dynamic Gd-DTPA MRI enhancement curve. *J Magn Reson.* 1993;Series B 102:129–136.
4. Antonetti DA, Barber AJ, Khin S, Lieth E, Tarbell JM, Gardner TW. Vascular permeability in experimental diabetes is associated with reduced endothelial occludin content: vascular endothelial growth factor decreases occludin in retinal endothelial cells. Penn State Retina Research Group. *Diabetes*. 1998;47:1953–1959.
5. DiMattio J. In vivo use of neutral radiolabeled molecular probes to evaluate blood-ocular barrier integrity in normal and streptozotocin-diabetic rats. *Diabetologia*. 1991;34:862–867.
6. Tilton RG, Weigel C, Eades D, Sherman WR, Kilo C, Williamson JR. Increased ocular blood flow and 125 I-albumin permeation in galactose-fed rats: inhibition by sorbinil. *Invest Ophthalmol Vis Sci*. 1988;29:861–868.
7. Xu Q, Qaum T, Adamis AP. Sensitive blood–retinal barrier breakdown quantitation using Evans blue. *Invest Opthalmol Vis Sci*. 2001;42:789–794.
8. Vinores SA, McGehee R, Lee A, Gadegbeku C, Campochiaro PA. Ultrastructural localization of blood–retinal barrier breakdown in diabetic and galactosemic rats. *J Histochem Cytochem*. 1990;38:1341–1352.
9. Caspers-velu LE, Wadhwani KC, Rapoport SI, Kador PF. Permeability of the blood–retinal and blood–aqueous barriers in galactose-fed rats. *J Ocul Pharmacol Ther*. 1995;11:469–487.
10. Ennis SR. Permeability of the blood– ocular barrier to mannitol and PAH during experimental diabetes. *Curr Eye Res*. 1990;9:827–838.
11. Ennis SR, Betz AL. Sucrose permeability of the blood–retinal and blood–brain barriers. Effects of diabetes, hypertonicity, and iodate. *Invest Ophthalmol Vis Sci*. 1986;27:1095–1102.
12. Lightman S, Rechthand E, Terubayashi H, Palestine A, Rapaport S, Kador P. Permeability changes in blood–retinal barrier of galactosemic rats are prevented by aldose reductase inhibitors. *Diabetes*. 1987;36:1271–1275.
13. Sander B, Larsen M, Engler C, Moldow B, Lund-Andersen H. Diabetic macular edema: the effect of photocoagulation on fluorescein transport across the blood–retinal barrier. *Br J Ophthalmol*. 2002;86:1139–1142.
14. Sander B, Larsen M, Engler C, et al. Diabetic macular edema: a comparison of vitreous fluorometry, angiography, and retinopathy. *Br J Ophthalmol*. 2002;86:316–320.
15. Sander B, Larsen M, Moldow B, Lund-Andersen H. Diabetic macular edema: passive and active transport of fluorescein through the blood-retina barrier. *Invest Ophthalmol Vis Sci*. 2001;42:433–438.
16. Grimes PA. Carboxyfluorescein distribution in ocular tissues of normal and diabetic rats. *Curr Eye Res*. 1988;7:981–988.
17. Grimes PA. Carboxyfluorescein transfer across the blood–retinal barrier evaluated by quantitative fluorescence microscopy: comparison with fluorescein. *Exp Eye Res*. 1988;46:769–783.
18. Grimes PA. Fluorescein distribution in retinas of normal and diabetic rats. *Exp Eye Res*. 1985;41:227–238.
19. Metrikin DC, Wilson CA, Berkowitz BA, Lam MK, Wood GK, Peshock RM. Measurement of blood–retinal barrier breakdown in endotoxin-induced endophthalmitis. *Invest Ophthalmol Vis Sci*. 1995;36:1361–1370.
20. Tofts PS, Berkowitz BA. Measurement of capillary permeability from the Gd enhancement curve: a comparison of bolus and constant infusion injection methods. *Magn Reson Imaging*. 1994;12:81–91.
21. Wood GK, Berkowitz BA, Wilson CA. Visualization of subtle contrast-related intensity change using temporal correlation. *Magn Reson Imaging*. 1994;12:1013–1020.
22. Ando N, Sen HA, Berkowitz BA, Wilson CA, de Juan E Jr. Localization and quantitation of blood–retinal barrier breakdown in experimental proliferative vitreoretinopathy. *Arch Ophthalmol*. 1994;112:117–122.
23. Berkowitz BA, Wilson CA, Tofts PS, Peshock RM. Effect of vitreous fluidity on the measurement of blood–retinal barrier permeability using contrast-enhanced MRI. *Magn Reson Med*. 1994;31:61–66.
24. Wilson CA, Fleckenstein JL, Berkowitz BA, Green ME. Preretinal neovascularization in diabetic retinopathy: a preliminary investigation using contrast-enhanced magnetic resonance imaging. *J Diab Comp*. 1992;6:223–229.
25. Berkowitz BA, Sato Y, Wilson CA, de Juan E. Blood–retinal barrier breakdown investigated by real-time magnetic resonance imaging after gadolinium-diethylenetriaminepentaacetic acid injection. *Invest Ophthalmol Vis Sci*. 1991;32:2854–2860.
26. Berkowitz BA, Tofts PS, Sen HA, Ando N, de Juan E Jr. Accurate and precise measurement of blood–retinal barrier breakdown using dynamic Gd-DTPA MRI. *Invest Ophthalmol Vis Sci*. 1992;33:3500–3506.
27. Vinores SA, Derevjanik NL, Mahlow J, Berkowitz BA, Wilson CA. Electron microscopic evidence for the mechanism of blood–retinal barrier breakdown in diabetic rabbits: comparison with magnetic resonance imaging. *Pathol Res Practice*. 1998;194:497–505.
28. Freeman ML, Barnes WE, Eastman G, et al. Radionuclide detection of blood–retinal barrier disruption in diabetes mellitus. *Semin Nucl Med*. 1984;14:16–20.
29. Anstadt B, Blair NP, Rusin M, Cunha-Vaz JG, Tso MO. Alteration of the blood–retinal barrier by sodium iodate: kinetic vitreous fluorophotometry and horseradish peroxidase tracer studies. *Exp Eye Res*. 1982;35:653–662.
30. Nilsson SEG, Knave B, Persson HE. Changes in ultrastructure and function of the sheep pigment epithelium and retina induced by sodium iodate. II. Early effects. *Acta Ophthalmol.* 1977;1007–1026.
31. Davson H, Hollingsworth JR. The effects of iodate on the blood–vitreous barrier. *Exp Eye Res*. 1972;14:21–28.
32. Taarnhoj J, Alm A. The effect of sodium iodate on the blood–retinal and blood–brain barriers. *Graef Arch Clin Exp Ophthalmol*. 1992;230:589–591.
33. Berkowitz BA, Lukaszew RA, Mullins CM, Penn JS. Impaired hyaloidal circulation function and uncoordinated ocular growth patterns in experimental retinopathy of prematurity. *Invest Ophthalmol Vis Sci*. 1998;39:391–396.
34. Pelc N. Optimization of flip angle for T1 dependent contrast in MRI. *Magn Reson Med*. 1993;29:695–699.
35. Gadian DG, Payne JA, Bryant DJ, Young IR, Carr DH, Bydder GM. Gadolinium-DTPA as a contrast agent in MR imaging: theoretical projections and practical observations. *J Comput Assist Tomog*. 1985;9:242–251.
36. Derevjanik NL, Vinores SA, Xiao WH, et al. Quantitative assessment of the integrity of the blood–retinal barrier in mice. *Invest Ophthalmol Vis Sci*. 2002;43:2462–2467.
37. Alikacem N, Yoshizawa T, Nelson KD, Wilson CA. Quantitative MR imaging study of intravitreal sustained release of VEGF in rabbits. *Invest Ophthalmol Vis Sci*. 2000;41:1561–1569.
38. Qaum T, Xu Q, Joussen AM, et al. VEGF-initiated blood retinal barrier breakdown in early diabetes. *Invest Opthalmol Vis Sci*. 2001;42:2408–2413.
39. Aiello LP, Bursell SE, Clermont A, et al. Vascular endothelial growth factor-induced retinal permeability is mediated by protein kinase C in vivo and suppressed by an orally effective beta-isoform-selective inhibitor. *Diabetes*. 1997;46:1473–1480.
40. Mathews MK, Merges C, McLeod DS, Lutty GA. Vascular endothelial growth factor and vascular permeability changes in human diabetic retinopathy. *Invest Ophthalmol Vis Sci*. 1997;38:2729–2741.
41. Lukaszew RA, Mullins CM, Penn JS, Berkowitz BA. Noninvasive and quantitative staging of hyaloidopathy in experimental retinopathy of prematurity. *Invest Ophthalmol Vis Sci*. 1997;38:S747.
42. Cunningham SA, Stephan CC, Arrate MP, Ayer KG, Brock TA. Identification of the extracellular domains of Flt-1 that mediate ligand interactions. *Biochem Biophys Res Commun*. 1997;231:596–599.
43. Cunningham SA, Tran TM, Arrate MP, Brock TA. Characterization of vascular endothelial cell growth factor interactions with the kinase insert domain-containing receptor tyrosine kinase. A real time kinetic study. *J Biol Chem*. 1999;274:18421–18427.
44. Lightman S, Pinter G, Yuen L, Bradbury M. Permeability changes at blood–retinal barrier in diabetes and effect of aldose reductase inhibition. *Am J Physiol*. 1990;259:R601–R605.

45. Enea NA, Hollis TM, Kern JA, Gardner TW. Histamine H1 receptors mediate increased blood–retinal barrier permeability in experimental diabetes. *Arch Ophthalmol*. 1989;107:270–274.
46. Murata T, Ishibashi T, Khalil A, Hata Y, Yoshikawa H, Inomata H. Vascular endothelial growth factor plays a role in hyperpermeability of diabetic retinal vessels. *Ophthalmic Res*. 1995;27:48–52.
47. Jones CW, Cunha-Vaz JG, Rusin MM. Vitreous fluorophotometry in the alloxan- and streptozocin-treated rat. *Arch Ophthalmol*. 1982; 100:1141–1145.
48. Dallal MM, Chang SW. Evans blue dye in the assessment of permeability-surface are product in perfused rat lungs. *J Appl Physiol*. 1994;77:1030–1035.
49. Menzies SA, Hoff JT, Betz AL. Extravasation of albumin in ischemic brain edema. *Acta Neurochir Suppl (Wien)*. 1990;51:220–222.
50. Nagy Z, Szabo M, Huttner I. Blood–brain barrier impairment by low pH buffer perfusion via the internal carotid artery in rat. *Acta Neuropathol (Berl)*. 1985;68:160–163.
51. Yi-Ming W, Shu H, Miao CY, Shen FM, Jiang YY, Su DF. Asynchronism of the recovery of baroreflex sensitivity, blood pressure, and consciousness from anesthesia in rats. *J Cardiovasc Pharmacol*. 2004;43:1–7.
52. Mayhan WG. Regulation of blood–brain barrier permeability. *Microcirculation*. 2001;8:89–104.